

Adaptive Object Detection Using Adjacency and Zoom Prediction

Yongxi Lu
 University of California, San Diego
 yol070@ucsd.edu

Tara Javidi
 University of California, San Diego
 tjavidi@ucsd.edu

Svetlana Lazebnik
 University of Illinois at Urbana-Champaign
 slazebni@illinois.edu

Abstract

State-of-the-art object detection systems rely on an accurate set of region proposals. Recent methods such as Multi-Box [5], YOLO [22] and RPN [23] use a single neural net evaluation to hypothesize promising object locations. While these approaches are computationally efficient, they rely on fixed image regions as anchors for predictions. In this paper we propose to use a search strategy that adaptively directs computational resources to sub-regions likely to contain objects. Compared to methods based on fixed anchor locations, our approach naturally adapts to cases where object instances are sparse and small. Our approach is comparable in terms of accuracy to the state-of-the-art Faster R-CNN approach while using two orders of magnitude fewer anchors on average.

1. Introduction

Object detection is an important computer vision problem for its intriguing challenges and the large variety of applications. Significant recent progress in this area has been achieved by incorporating deep convolutional neural networks (DCNN) [16] in object detection systems [27, 10, 5, 12, 18, 25, 26, 8]. In particular, approaches based on region-based features [10] have achieved groundbreaking results on standard object detection benchmarks.

An object detection algorithm with state-of-the-art accuracy typically has the following two-step cascade. As a first step, a set of class-independent region proposals are hypothesized either by low-level image features [29, 31, 1, 14] or a deep network specifically trained for this purpose [5, 23]. These proposed regions are then used as input to a detector that gives each region a class label. The role of region proposal is to reduce the complexity through limiting the number of regions that need be evaluated by the detector. However, with recently introduced techniques that enable shar-

ing of convolutional features [12, 9], traditional region proposals algorithms such as selective search [29] and Edge-Boxes [31] become the bottleneck of the detection pipeline.

An emerging class of region proposal methods based on an end-to-end trained deep neural network have provided promising leads towards real-time multi-class object detection [5, 23]. The common idea in these approaches are to train class-independent regressor on a small set of pre-defined anchor regions. More specifically, each anchor region is assigned the task of deciding whether an object is in its neighborhood (in terms of center location, scale and aspect ratio), and predicting a bounding box for that object through regression if that is the case. We note that these algorithms can successfully detect an object at test time only if one of the anchor regions is in its neighborhood. Essentially, the definition of anchor regions encodes prior beliefs on typical object whereabouts. While these approaches have performed well on standard object detection benchmarks, they may not generalize to real-world situations. The large-scale datasets for which these algorithms are designed are typically collected from results of Internet search engines [7, 24, 19]. The fact that Internet images are originally captured for the purpose of display and appreciation intrinsically biases towards large objects at central locations. Anchor regions designed to work for such a dataset could be fundamentally flawed when tested on images captured for other applications. Using an exhaustive set of anchors at different locations, sizes and aspect ratios may result in a more robust algorithm, but that comes with the cost of excessive computational complexity.

We alternatively consider the following adaptive search strategy. Instead of deciding a priori a set of anchor regions, our algorithm starts with the entire image. It then recursively divides the image into sub-regions (see Figure 3) until it is unlikely for a given region to enclose any small objects. The regions that are visited in the process effectively serve as anchors which are assigned the task of predicting

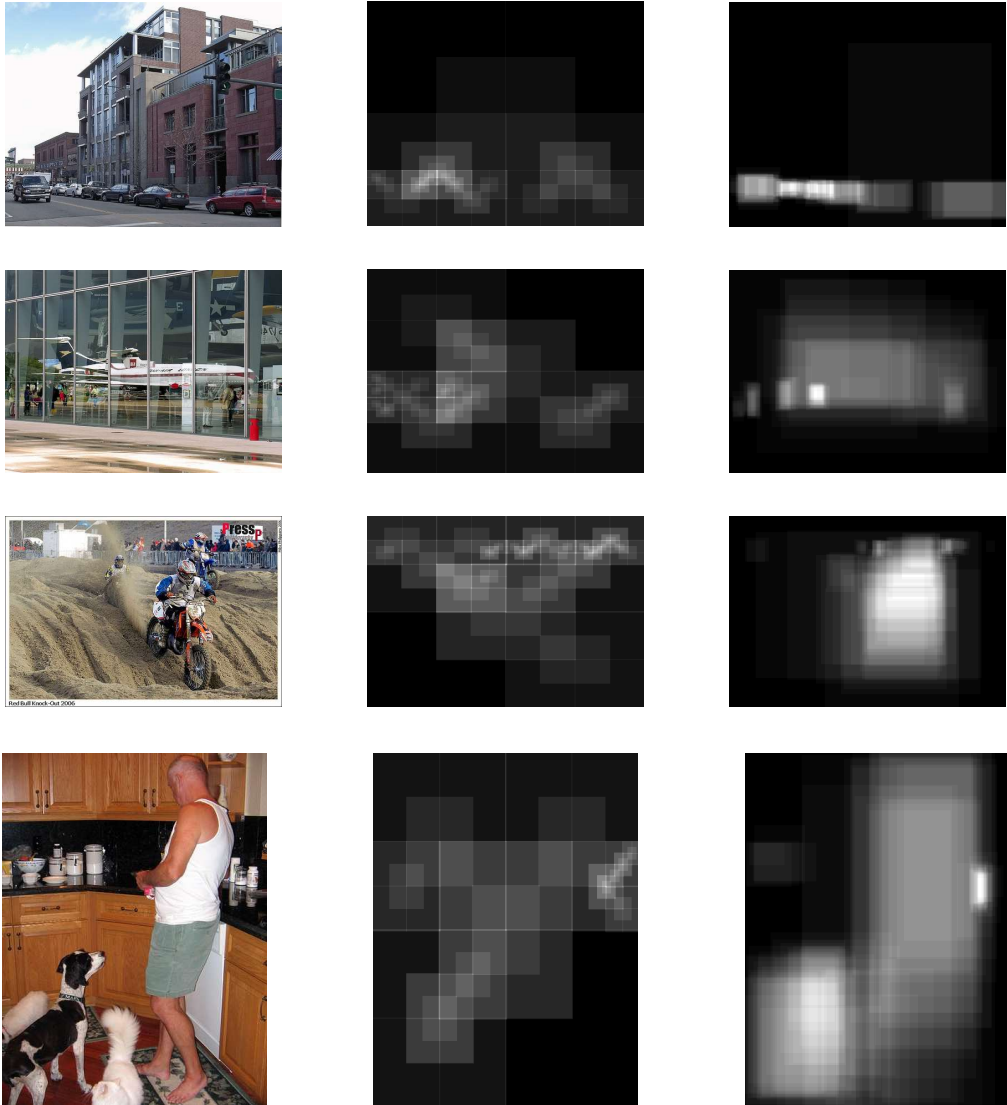


Figure 1. Example outputs of our algorithm. Left column shows the original image. The middle column shows the effective anchor regions induced by our adaptive search. The right column shows the top-100 adjacency predictions made around the anchor regions. The anchor regions and the adjacency predictions are superimposed into a figure at the same resolution of the original image. We note that the anchor regions and the region proposals in our approach are shared across object categories. For the last example the algorithm generates anchor regions at proper scales near the dogs, the person and the bottles.

object bounding boxes for objects nearby. A salient feature of our algorithm is that the decision of whether to divide a region further is based on features extracted at that particular region. As a result the generation of the set of effective anchor regions are conditioned on the image content. For an image with only a few small objects most regions are pruned early in the search, leaving a few small anchor regions near the objects. For images that contain exclusively large instances, our approach gracefully falls back to existing methods that rely on a small number of large anchor

regions. In this manner, our algorithm adaptively directs its computational resources to regions that are likely to contain objects. Figure 1 shows on a set of example images the anchor regions and adjacency predictions produced by our algorithm. Note that the small anchor regions generated by our algorithm are concentrated at regions where small objects are present.

The success of this approach is contingent upon two essential observations. Firstly, observing features from large entities could strongly indicate the existence of a smaller

high resolution entity. Secondly, it is possible to infer about the contents of a region if features from an overlapping adjacent regions are available. To provide intuitive evidence for these observations, consider for example the process of a human searching for a car in an image. One successful strategy is to first look for large structures, such as roads and highways. Note that although these structures are class-dependent, the same large structures could provide strong contexts to instances from supercategories, such as ground vehicles. Observing these structures quickly shrink the search space since we know from daily experience that cars drive on these surfaces. This strategy can be improved further if we use the fact that seeing part of the car, such as an engine cover, could give us rich information about the spatial support of the rest of the car. This enables a more coarse search with the equivalent detection accuracy.

Motivated by these key observations, we design heuristics to support our adaptive search algorithm. In particular, we train a deep neural network called Adjacency and Zoom Network (AZ-Net) using pre-trained DCNN features. The AZ-Net relies on the spatial correlation among sub-regions of an image to output two quantities for an input region. The first quantity is a scalar called *zoom indicator* which is used to decide whether to further zoom (divide) into the region. The second quantity is a set of bounding-boxes with confidence scores called *adjacency predictions*. The adjacency predictions with high confidence scores are then used as region proposals for a subsequent object detector.

We evaluate our full detection pipeline on standard image datasets. In particular, we compare the accuracy of our algorithm on Pascal VOC 2007 [6] and extensively evaluate various aspects of our approach. We also report baseline results on the newly introduced MSCOCO [19] dataset. Our algorithm achieves detection mAP that is close to state-of-the-art methods at a fast frame rate.

In summary, we make the following contributions:

- We design an adaptive search strategy for object detection that naturally handles cases where object instances are sparse and small, and yet falls back to existing successful strategy when the object instances are large.
- We evaluate our approach on standard image datasets and demonstrate its effectiveness in object detection using standard metrics.
- We provide a fine-grained analysis that shows intriguing features of our approach. Namely, our proposal strategy has better recall for higher intersection-over-union thresholds, higher recall for smaller numbers of top proposals, and for smaller object instances.

This paper is organized as follows. In section 2 we survey existing works in the literature highlighting the novelty of our approach. In Section 3 we introduce the design of

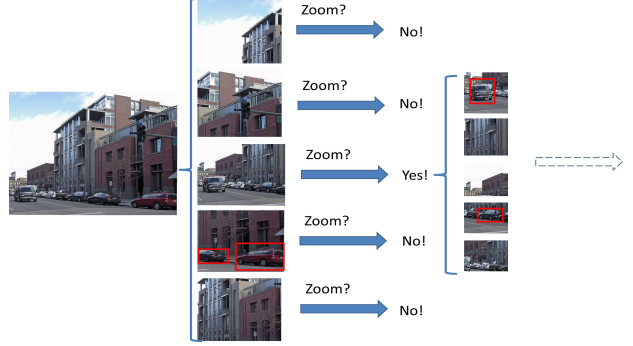


Figure 2. Illustration of the pipeline of our algorithm using an example. The red boxes shows region proposals from adjacency predictions. A region that contains small objects is further divided into sub-regions, and the same procedure continues recursively until the zoom indicator is below threshold or the region itself is too small.

our algorithm. In particular, we discuss the intuition and design of the essential building blocks. These observations are reflected in the our implementation, which is discussed in Section 4. The empirical comparison to existing object detection methods on standard evaluation benchmarks are discussed in Section 5. We conclude our paper and discuss possible future directions in Section 6.

2. Previous Works

Our work is related to Lampert *et al.* [17] which uses a branch-and-bound approach that induces an interesting sequential search structure for object detection. However, their approach is restricted to a particular set of object detectors and cannot take advantage of the more accurate DCNN-based detectors. The idea of using sequential search for object localization has also been explored from a theoretical perspective in [21]. More recently, Gonzeles-Garcia *et al.* [11], Caicedo and Lazebnik [3], and Yoo *et al.* [30] explores active object detection with DCNN features. While these approaches reveal intriguing benefits of using an adaptive algorithm for object detection, their detectors are class-wise and their methods cannot achieve competitive accuracy. Our approach on the other-hand is multi-class and is comparable to state-of-the-art approaches in both accuracy and test speed.

The idea of using spatial context has been previously explored in the literature. Previous work by Torralba *et al.* [28] uses a biologically inspired visual attention [2] model, but our focus is on efficient engineering design. Divvala *et al.* [4] also propose to use context for localization, but their empirical study was performed on hand-crafted features and need to be reexamined when combined with more accurate recent approaches. The more recent work by Lu and Javidi [20] uses spatial correlation to guide DCNN-based object

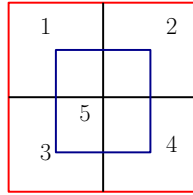


Figure 3. As illustrated, a given region is divided into 5 sub-regions (numbered). Each of these sub-regions is recursively divided if its zoom indicator is above a threshold.

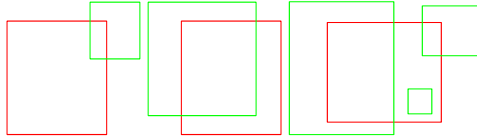


Figure 4. Illustration of desired zoom indicator at common situations. The green boxes are objects, and the red boxes are regions. Left: the object is small, but it is mostly outside the region, there is on gain in zooming in. Middle: the object is mostly inside, but its size is large relative to the region, there is no gain in zooming in. Right: there is a small object that is completely inside the region, in this case further division of the region greatly increases the chance of detection for that object.

detectors, but their method is complicated and the contribution of adaptivity is unclear. Furthermore, their approach has not been evaluated on standard object detection benchmarks.

Our approach is closely related to recent approaches that use anchor regions for proposal generation or detection. For example, Erhan *et al.* [5] use 800 data-driven anchors for region proposals and Redmon *et al.* [22] use a fixed grid of 49 non-overlapping regions to provide class-wise detections. The former has the concern that these anchors could overfit the data, while the latter cannot achieve state-of-the-art performance without model ensembles. Our work is most related to the recent work by Ren *et al.* [23] which uses a set of heuristically designed 2400 overlapping anchor regions. Our approach uses a similar regression technique to predict multiple bounding boxes from an anchor region. However, our anchor regions are generated adaptively, making them intrinsically more efficient. In particular, we offer an answer to the following question: is it possible to detect small object instances in the scene without an excessive number of anchor regions? Our answer is affirmative: we propose to grow a tree of finer-grained anchor regions based on local image evidence, and design the regression model strategically on top of it. We extensively compare the output of our method against [23] in our experiment section and shows the unique advantages of our approach.

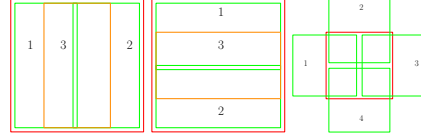


Figure 5. Illustration of sub-region templates. From left to right: vertical stripes, horizontal stripes, neighboring squares. The red rectangular box is the image. In the figure the regions labeled by number are template sub-regions. The gaps between sub-regions are exaggerated for better visualization. The vertical stripes are used to detect tall objects, the horizontal stripes are used to detect fat objects, while the neighboring squares are used to detect objects that fall in the gaps between anchor regions generated in the search process.

3. Design of the Algorithm

In this section we introduce the design of our algorithm. We first give an overview of our approach. This is followed by a discussion on the design of building blocks and their roles in our algorithm.

3.1. Overview of the Adaptive Search

Our object detection algorithm consists of two steps. In step 1, a set of class-independent region proposals are generated in an adaptive search algorithm called Adaptive Search with AZ-Net (see Algorithm 1). In step 2, an object detector evaluates each region proposed in step 1 to provide class-wise detections.

Our focus is on improving step 1. We consider a recursive search strategy, starting from the entire image as the root region. Consider any particular region encountered in the search procedure. The algorithm extracts features from this region to compute the zoom indicator and the adjacency predictions. On the one hand, the adjacency predictions with confidence scores above a threshold is included in the set of output region proposals. On the other hand, if the zoom indicator is above a manually set threshold, this indicates that the current region is likely to contain small objects. To detect these embedded small objects, the current region is divided into sub-regions in the manner shown in Figure 3. Each of these sub-regions is then recursively processed in the same manner as its parent region, until either its area or its zoom indicator is too small. An example illustrating the procedure can be seen in Figure 2.

Clearly, the essential elements of our algorithm are the zoom indicator and the adjacency prediction. We will discuss their design in the next section.

3.2. Design of Building Blocks

In our algorithm, the zoom indicator directs search towards regions with small objects, while the adjacency prediction detects objects that are near the current region. Since

Algorithm 1: Adaptive search with AZ-Net

Data: Input image x (the whole image region b_x). Y_k is the region proposed at step k . Y^k is the accumulated region proposals up to step k . Z_k is regions to further zoom in at step k . B_k are anchor regions at step k .

Result: Region proposals at termination Y^K

Initialization: $B_0 \leftarrow \{b_x\}$. $Y^0 \leftarrow \emptyset$, $k \leftarrow 0$.

while (B_k is not an empty set) **do**

- Initialize Y_k and Z_k as empty sets.
- foreach** $b \in B_k$ **do**

 - Compute adjacency predictions A_b and the zoom indicator z_b using AZ-Net
 - Include all $a \in A_b$ with high confidence scores into Y_k
 - Include b into Z_k if z_b is above threshold

- end**
- $Y^k \leftarrow Y^{k-1} \cup Y_k$
- $B_{k+1} \leftarrow \text{Divide-Regions}(Z_k)$
- $k \leftarrow k + 1$

end

$K \leftarrow k - 1$

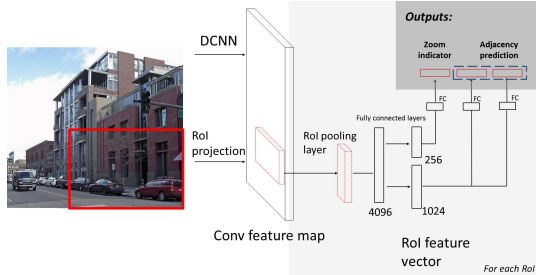


Figure 6. Illustration of the AZ-Net architecture.

the two tasks are intrinsically related, the design of these two components are jointly considered.

In particular, the zoom indicator should be large for a region only when there exists at least one object with the following properties. Firstly, the spatial support of the object should mostly lie within the region. Secondly, the size of the object should be sufficiently small compared to the size of the region. The reasoning underlying this design is that we should zoom in to the a region only when it substantially increases the chance of detection. For example, if an object is mostly outside the region, dividing the region further is unlikely to increase the chance of detecting that object. Similarly, if an object is large compared to the current region, the task of detecting this object should be handled by this region or its parents. In the latter case, further division of the region not only wastes computational resources, but also introduces false positives in the region proposals. Figure 4 shows common situations and the desirable behavior of the zoom indicator.

The role of adjacency prediction is to detect one or multiple objects that overlaps with the anchor region sufficiently

by providing tight bounding boxes. The adjacency prediction should be aware of the search geometry induced by the zoom indicator. More specifically, the adjacency prediction should perform well on the effective anchor regions induced by the search algorithm. For this purpose we propose a training procedure that is aware of the adaptive search scheme (discussed in Section 4). On the other hand, its design should explicitly account for typical geometric configurations of objects that fall inside the region, so that the training can be performed in consistent fashion. For this reason, we propose to make predictions based on a set of sub-region templates as shown in Figure 5. We note that we make sub-region templates large on purpose. Our intuition is that if an object is small, a good strategy is to first zoom in and make predictions only when the features extracted at smaller regions are available.

4. Implementation

We implement our algorithm using the Caffe [15] framework, utilizing the open source infrastructure provided by the Fast R-CNN repository [9]. In this section we introduce the implementation details of our approach, including the architecture and training procedures of the AZ-Net and the Fast R-CNN detector. We note that we use Fast R-CNN detector since it is a fast and accurate recent approach. Our method should in principle work for a broader class of object detectors that use region proposals.

4.1. Adjacency and Zoom Network (AZ-Net)

As discussed in previous sections, the AZ-Net provides heuristics that supports the adaptive search algorithm. In particular, given an image and an input region, the AZ-Net provides a scalar zoom indicator and a set of bound-

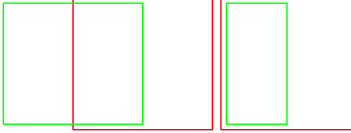


Figure 7. Illustration of the inverse matching procedure. The red box is the inverse matching of the object (green box). The left figure shows inverse matching of a neighboring square, the right figure shows inverse matching of a vertical stripe.

ing boxes with their confidence scores which is called adjacency predictions.

Since the zoom indicator and adjacency predictions encode high level visual concepts, we train a deep neural network as illustrated in Figure 6. Note that in addition to the sub-region templates as shown in Figure 5, we also add the region itself as a special sub-region, making in total 11 adjacency predictions per image. For the convolutional layers, we use the VGG16 model [25] pre-trained on ImageNet data. The fully-connected layers are on top of a region pooling layer introduced in [9] which allows efficient sharing of convolutional layer features.

The training is performed as a three step procedure. Firstly, a set of regions are sampled from the image. These samples should contain hard positive and negative examples for both the zoom indicator and the adjacency prediction. These samples are then labeled based on the ground truth object annotations and the design requirements as discussed in Section 3. Finally, the tuples of samples and labels are used in standard stochastic gradient descent training. Since the success of our algorithm is contingent upon a proper training procedure, we now discuss how the regions are sampled and labeled, and the loss function we choose.

4.1.1 Region Sampling

Since a typical image only has a few object instances, to provide sufficient positive examples for adjacency predictions our method inversely finds regions that will see a ground truth object as a perfect fit to its template sub-regions (see Figure 7 for illustration). This provides $k \times 11$ training examples for each image, where k is the number of objects.

To provide examples for the zoom indicator, we search an input image as in Algorithm 1. Since the zoom indicator is not initially available, we replace it with a noisy version of the ground truth zoom indicator label (to be defined later). We use the regions that are zoomed in (Z_k in Algorithm 1) as training examples. For training zoom indicators, these regions are more informative as they are close to the objects. For training the adjacency predictions, these regions typically provide difficult positive and negative examples and they are closer to the regions encountered in

test time. We use noisy zoom labels (randomly flipping the zoom labels) to diversify the training examples. For each input image we initiate this procedure at 5 sub-images and repeat it at multiple times. This procedure samples around 2000 regions per image on Pascal dataset.

We also append horizontally flipped images to the dataset for data augmentation. In those cases due to the randomness of the noisy zoom indicators the sampled regions for a horizontally flipped pair of images may not be symmetric to each other.

4.1.2 Region Labeling

The label for zoom indicator follows the discussion in 3. The label is 1 if there exists an object with 50% inside the region and at most 25% of the size of the region. For adjacency prediction, we set a threshold in the intersection-over-union (IoU) score between an object and a region. A region is assigned to detect objects with sufficient overlapping. The assigned objects are then greedily matched to one of the sub-regions defined by the templates shown in Figure 5. The priority in the matching is determined by the IoU score between the objects and the sub-regions. We note that in this manner multiple predictions from a region is possible.

4.1.3 Loss Function

As shown in Figure 6, the AZ-Net has three output layers. The zoom indicator outputs from a sigmoid activation function. Naturally we use cross-entropy loss function popular for binary classification. For the adjacency predictions, the bounding boxes are parameterized as in Fast R-CNN [23]. Unlike in Fast R-CNN, to provide multiple predictions from any region the output of the confidence scores are not normalized to a probability vector. Correspondingly we use smooth L1-loss for bounding boxes output and element-wise cross-entropy loss for confidence scores output. The loss from three layers are summed together to form a multi-task loss function.

4.2. Fast R-CNN Training

To prepare the Fast R-CNN detector, we mostly follow the training procedure introduced in [9]. However, instead of using selective search regions from images, we use the regions proposed by AZ-Net. To provide a diverse set of examples, we rank the generated proposals in the order of their confidence scores and select the top 2000. We note that we set a particularly low threshold in the zoom indicator to ensure there is enough proposals. These regions are augmented by the ground truth boxes as strong positive examples. Finally, we augment the dataset with horizontally flipped images.

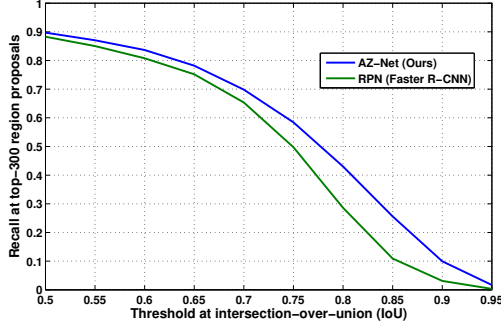


Figure 8. Comparison of recall of region proposals generated by AZ-Net and RPN at different intersection over union thresholds on VOC 2007 test. The comparison is performed at top-300 region proposals. Our approach has better recall at large IoU threshold, which suggests AZ-Net proposals are more accurate in localizing the objects.

5. Experiments

We extensively evaluate our approach on Pascal VOC 2007 [6] dataset. The Pascal VOC 2007 results are prepared by using the toolkit provided in [6]. In addition to high level object detection results, we also perform detailed comparison between the RPN approach adopted in Faster R-CNN and our AZ-Net. This shows several advantages of our approach. We also evaluate our method on the MSCOCO [19] dataset. This section is concluded by an analysis on the efficiency of our adaptive search strategy.

5.1. Results on VOC 2007

To set up a baseline comparison, we evaluate our approach using the standard average precision (AP) metric for object detection. For AP evaluation we use the development kit provided by the VOC 2007 object detection challenge. Our models for VOC 2007 are trained 80k iterations with a mini-batch size of 128 regions and one image per mini-batch. We compare our approach against the recently introduced Fast R-CNN [9] and Faster R-CNN [23] object detection systems. These systems achieve state-of-the-art performance in standard object detection benchmarks, such as VOC 2007 [6] and VOC 2012 [7]. A comparison is shown in Table 1. The results suggest that our approach is comparable to or better than these state-of-the-art methods.

5.2. Quality of Region Proposals

We perform a detailed analysis of the quality of region proposals from our AZ-Net, highlighting a comparison to the state-of-the-art RPN network used in Faster R-CNN. For all our experiments, we analyze the recall on Pascal VOC 2007 test set using the following definition of recall: An object is counted as retrieved if there exists a region proposal with an above-threshold IoU with it. The recall is then calculated as the proportion of the retrieved objects among all ground truth object instances. To accurately reproduce the RPN approach, we download the region proposals provided on the Faster R-CNN repository¹. We use the results from a model reportedly trained on VOC 2007 trainval. Correspondingly we compare it against our model trained on VOC 2007 trainval set. The comparison concerning top-N regions are performed by ranking the region proposals in the order of their confidence scores. We note that the region proposal results from RPN come with confidence scores.

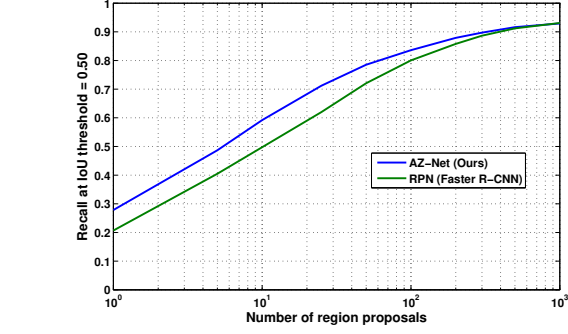


Figure 9. Comparison of recall of region proposals generated by AZ-Net and RPN at different number of region proposals on VOC 2007 test. The comparison is performed at IoU threshold 0.5. Our approach has better early recall. In particular, it reaches 0.6 recall with only 10 proposals.

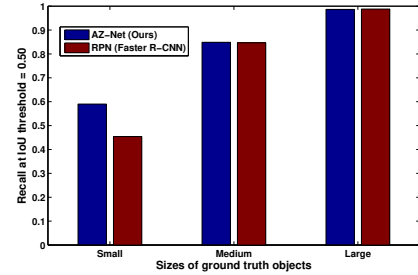


Figure 10. Comparison of recall of region proposals generated by AZ-Net and RPN for objects in different sizes on VOC 2007 test. The comparison is performed at IoU threshold 0.5 with top-300 proposals. Our approach has significantly better recall for small objects.

posal with an above-threshold IoU with it. The recall is then calculated as the proportion of the retrieved objects among all ground truth object instances. To accurately reproduce the RPN approach, we download the region proposals provided on the Faster R-CNN repository¹. We use the results from a model reportedly trained on VOC 2007 trainval. Correspondingly we compare it against our model trained on VOC 2007 trainval set. The comparison concerning top-N regions are performed by ranking the region proposals in the order of their confidence scores. We note that the region proposal results from RPN come with confidence scores.

Figure 8 shows a comparison of recall at different IoU thresholds. Recalls reported at a higher IoU threshold is indicative of the localization accuracy of a set of region proposals. We note that our AZ-Net approach outperforms RPN in this comparison. This suggests our method generates bounding boxes that in general overlap with the ground truth objects better.

¹https://github.com/ShaoqingRen/faster_rcnn

Method	mAP	aero	bike	bird	boat	bottle	bus	car	cat	chair	cow	table	dog	horse	mbike	person	plant	sheep	sofa	train	tv
AZ-Net (ours)	69.6	74.8	78.6	67.9	57.9	50.4	82.5	80.9	84.3	43.1	77.5	65.7	81.3	83.8	76.8	75.9	35.6	67.8	64.5	77.9	65.4
RPN-shared	69.9	70.0	80.6	70.1	57.3	49.9	78.2	80.4	82.0	52.2	75.3	67.2	80.3	79.8	75.0	76.3	39.1	68.3	67.3	81.1	67.6
RPN-unshared	68.5	74.1	77.2	67.7	53.9	51.0	75.1	79.2	78.9	50.7	78.0	61.1	79.1	81.9	72.2	75.9	37.2	71.4	62.5	77.4	66.4
Fast R-CNN	68.1	74.6	79.0	68.6	57.0	39.3	79.5	78.6	81.9	48.0	74.0	67.4	80.5	80.7	74.1	69.6	31.8	67.1	68.4	75.3	65.5

Table 1. Comparison on VOC 2007 test set using VGG-16 for convolutional layers. The results of RPN are reported at [23]. The results for Fast R-CNN are reported in [9]. For our results the convolutional layers of the AZ-Net and the Fast R-CNN detector are unshared. The AZ-Net and RPN results are reported for 300 region proposals. The Fast R-CNN method uses approximately 2000 region proposals generated by selective search. The RPN-shared method enables sharing of the convolutional features through alternating optimization. All listed methods use DCNN models trained on VOC 2007 trainval.

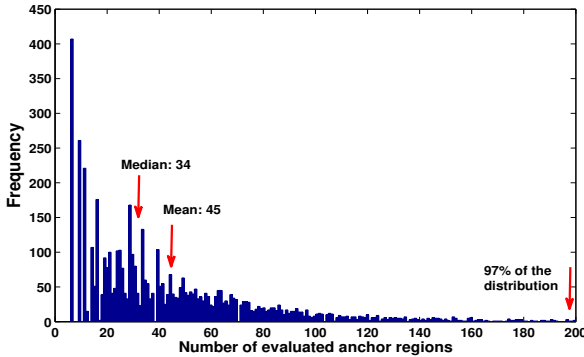


Figure 11. Distribution of the number of anchor regions evaluated on VOC 2007 test set. For most images a few dozens of anchor regions are required. Note that the anchor regions are shared across object categories.

We show in Figure 9 a plot of recall using top-N proposals. A region proposal algorithm is more efficient in covering objects if its area under curve is larger. Our experiment suggests that our AZ-Net approach has a better early recall than RPN. That means our algorithm in general can recover more objects with the same number of region proposals.

We also show in Figure 10 a comparison of recall for object with different sizes. For the division of sizes, we use the approach adopted in the evaluation criteria of MS COCO [19]. More specifically, the “small object” has an area less than 32^2 , a “medium object” has an area between 32^2 and 96^2 , a large object has an area greater than 96^2 . Our approach achieves higher recall on the small object subset. We note that this is because when small objects are present in the scene our adaptive search strategy generates small anchor regions strategically around them, as shown in Figure 1.

5.3. Efficiency of Adaptive Search

Our approach is efficient in runtime, as shown in Table 2. We note that this is achieved even with several severe inefficiencies in our implementation. Firstly, our current implementation requires separated convolutional layer computation for the AZ-Net and the Fast R-CNN detector, while in the Faster R-CNN (RPN) approach a simple alternating

Method	Anchor Regions	Region proposals	Runtime (ms)
AZ-Net (ours)	45	300	245
RPN (shared)	2400	300	198
RPN (unshared)	2400	300	342
Fast R-CNN	N/A	2000	1830

Table 2. Numbers related to the efficiency of the object detection methods listed in Table 1. The runtime for RPN and Fast R-CNN are reported for a K40 GPU [23]. Our runtime experiment is performed on a GTX 980Ti GPU. The K40 GPU has larger GPU memory, while the GTX 980Ti has higher clock rate.

optimization technique is introduced to allow sharing of the convolutional layer. We note that this technique is compatible to our approach. Secondly, for each image our algorithm requires several rounds of fully connected layer evaluation that induces expensive memory transfer between GPU and CPU. Thirdly, the Faster R-CNN approach uses convolutional computation for the evaluation of anchor regions, which are highly optimized compared to the ROI pooling technique we adopted. We note that despite these inefficiencies, our approach still achieves high accuracy at a state-of-the-art frame rate. This is due to the intrinsic efficiency from the adaptive search. With improved implementation our algorithm could be faster still.

The efficiency of our approach is due to the small number of anchor regions to evaluate. To further understand this aspect of our algorithm, we show in Figure 11 the distribution of anchor regions evaluated. For most images our method only require a few dozens of anchor regions. This number is much smaller than the 2400 anchor regions used in RPN [23] and the 800 used in MultiBox [5]. In addition, unlike class-specific search methods widely used in previous adaptive object detection schemes [3, 30] our anchor regions are class-generic, making it efficient for multi-class detection.

5.4. Results on MSCOCO

We also evaluate our method on MSCOCO dataset and submit the “UCSD” entry to the MSCOCO 2015 detection challenge. Our post-competition work shows that training the models with sufficient iterations is critical for good detection accuracy. In Table 3 we show the progression of accuracy as we increase the number of training iterations.

Our best post-competition model have an mAP of 0.223, which is outperformed by the winning “MSRA” entry with

Method	Iterations	AP	AP IoU=0.50	AP IoU=0.75	AP small	AP medium	AP large	AR max=1	AR max=10	AR max=100	AR small	AR medium	AR large
Fast R-CNN	240k	0.197	0.359	0.199	0.035	0.188	0.346	0.214	0.295	0.298	0.077	0.322	0.502
AZ-Net	240k+400k	0.188	0.369	0.176	0.035	0.188	0.315	0.206	0.303	0.313	0.090	0.342	0.519
AZ-Net	480k	0.206	0.388	0.200	0.045	0.204	0.339	0.216	0.319	0.328	0.108	0.356	0.527
AZ-Net	720k	0.223	0.410	0.218	0.049	0.221	0.368	0.229	0.335	0.345	0.115	0.376	0.555

Table 3. The detection mAP on MSCOCO 2015 test-dev set. The results are shown in chronological order, with the top AZ-Net entry being our submission to the MSCOCO 2015 detection challenge. The Fast R-CNN result is cited from [9]. A comparison to more recent methods can be found in <http://mscoco.org/dataset/#detections-leaderboard>.

an mAP of 0.373. Their approach is a Faster R-CNN style detection pipeline, replacing the VGG-16 network with an ultra-deep architecture called Deep Residual Network [13]. They also report significant improvement by model ensembles and using global contextual information. We note that these techniques are complementary to our approach and can be incorporated into our pipeline. Less aggressive modifications of network architecture are used in other top entries of the competition with detailed descriptions, addressing the importance of improving network design.

6. Conclusion and Future Work

In this paper we introduce an adaptive object detection system using adjacency and zoom predictions. Our algorithm adaptively focuses its computational resources to small regions likely to contain objects. To achieve this we propose to use spatial correlation between visual features in a strategic manner. In particular we design and train an Adjacency and Zoom Network (AZ-Net) that provides accurate search heuristics. Our system achieves state-of-the-art accuracy at a fast frame rate.

Our findings also open new possibilities for efficient detection of small objects. For instance, for high resolution images it is possible to use our search structure to focus high resolution convolutional layer computation to smaller regions. This could further improve efficiency and accuracy for detection of small objects.

References

- [1] P. Arbelaez, J. Pont-Tuset, J. Barron, F. Marques, and J. Malik. Multiscale combinatorial grouping. In *Computer Vision and Pattern Recognition (CVPR), 2014 IEEE Conference on*, pages 328–335. IEEE, 2014.
- [2] A. Borji and L. Itti. State-of-the-art in visual attention modeling. *Pattern Analysis and Machine Intelligence, IEEE Transactions on*, 35(1):185–207, 2013.
- [3] J. C. Caicedo and S. Lazebnik. Active object localization with deep reinforcement learning. *International Conference on Computer Vision (ICCV)*, 2015, to appear.
- [4] S. K. Divvala, D. Hoiem, J. H. Hays, A. Efros, M. Hebert, et al. An empirical study of context in object detection. In *Computer Vision and Pattern Recognition, 2009. CVPR 2009. IEEE Conference on*, pages 1271–1278. IEEE, 2009.
- [5] D. Erhan, C. Szegedy, A. Toshev, and D. Anguelov. Scalable object detection using deep neural networks. In *Computer Vision and Pattern Recognition (CVPR), 2014 IEEE Conference on*, pages 2155–2162. IEEE, 2014.
- [6] M. Everingham, L. Van Gool, C. K. I. Williams, J. Winn, and A. Zisserman. The PASCAL Visual Object Classes Challenge 2007 (VOC2007) Results. <http://www.pascal-network.org/challenges/VOC/voc2007/workshop/index.html>.
- [7] M. Everingham, L. Van Gool, C. K. I. Williams, J. Winn, and A. Zisserman. The PASCAL Visual Object Classes Challenge 2012 (VOC2012) Results. <http://www.pascal-network.org/challenges/VOC/voc2012/workshop/index.html>.
- [8] S. Gidaris and N. Komodakis. Object detection via a multi-region & semantic segmentation-aware cnn model. *arXiv preprint arXiv:1505.01749*, 2015.
- [9] R. Girshick. Fast r-cnn. *arXiv preprint arXiv:1504.08083*, 2015.
- [10] R. Girshick, J. Donahue, T. Darrell, and J. Malik. Rich feature hierarchies for accurate object detection and semantic segmentation. In *Computer Vision and Pattern Recognition (CVPR), 2014 IEEE Conference on*, pages 580–587. IEEE, 2014.
- [11] A. Gonzalez-Garcia, A. Vezhnevets, and V. Ferrari. An active search strategy for efficient object class detection. In *Proceedings of the IEEE Conference on Computer Vision and Pattern Recognition*, pages 3022–3031, 2015.
- [12] K. He, X. Zhang, S. Ren, and J. Sun. Spatial pyramid pooling in deep convolutional networks for visual recognition. In *Computer Vision–ECCV 2014*, pages 346–361. Springer, 2014.
- [13] K. He, X. Zhang, S. Ren, and J. Sun. Deep residual learning for image recognition. *arXiv preprint arXiv:1512.03385*, 2015.
- [14] A. Humayun, F. Li, and J. M. Rehg. Rigor: Reusing inference in graph cuts for generating object regions. In *Computer Vision and Pattern Recognition (CVPR), 2014 IEEE Conference on*, pages 336–343. IEEE, 2014.
- [15] Y. Jia, E. Shelhamer, J. Donahue, S. Karayev, J. Long, R. Girshick, S. Guadarrama, and T. Darrell. Caffe: Convolutional architecture for fast feature embedding. *arXiv preprint arXiv:1408.5093*, 2014.
- [16] A. Krizhevsky, I. Sutskever, and G. E. Hinton. Imagenet classification with deep convolutional neural networks. In *Advances in neural information processing systems*, pages 1097–1105, 2012.
- [17] C. H. Lampert, M. B. Blaschko, and T. Hofmann. Efficient subwindow search: A branch and bound framework for object localization. *Pattern Analysis and Machine Intelligence, IEEE Transactions on*, 31(12):2129–2142, 2009.

- [18] X. Liang, S. Liu, Y. Wei, L. Liu, L. Lin, and S. Yan. Computational baby learning. *arXiv preprint arXiv:1411.2861*, 2014.
- [19] T.-Y. Lin, M. Maire, S. Belongie, J. Hays, P. Perona, D. Ramanan, P. Dollár, and C. L. Zitnick. Microsoft coco: Common objects in context. In *Computer Vision–ECCV 2014*, pages 740–755. Springer, 2014.
- [20] Y. Lu and T. Javidi. Efficient object detection for high resolution images. *arXiv preprint arXiv:1510.01257*, 2015.
- [21] M. Naghshvar and T. Javidi. Two-dimensional visual search. In *Information Theory Proceedings (ISIT), 2013 IEEE International Symposium on*, pages 1262–1266. IEEE, 2013.
- [22] J. Redmon, S. Divvala, R. Girshick, and A. Farhadi. You only look once: Unified, real-time object detection. *arXiv preprint arXiv:1506.02640*, 2015.
- [23] S. Ren, K. He, R. Girshick, and J. Sun. Faster r-cnn: Towards real-time object detection with region proposal networks. *arXiv preprint arXiv:1506.01497*, 2015.
- [24] O. Russakovsky, J. Deng, H. Su, J. Krause, S. Satheesh, S. Ma, Z. Huang, A. Karpathy, A. Khosla, M. Bernstein, A. C. Berg, and L. Fei-Fei. ImageNet Large Scale Visual Recognition Challenge. *International Journal of Computer Vision (IJCV)*, pages 1–42, April 2015.
- [25] K. Simonyan and A. Zisserman. Very deep convolutional networks for large-scale image recognition. *arXiv preprint arXiv:1409.1556*, 2014.
- [26] C. Szegedy, W. Liu, Y. Jia, P. Sermanet, S. Reed, D. Anguelov, D. Erhan, V. Vanhoucke, and A. Rabinovich. Going deeper with convolutions. *arXiv preprint arXiv:1409.4842*, 2014.
- [27] C. Szegedy, A. Toshev, and D. Erhan. Deep neural networks for object detection. In *Advances in Neural Information Processing Systems*, pages 2553–2561, 2013.
- [28] A. Torralba, A. Oliva, M. S. Castelhano, and J. M. Henderson. Contextual guidance of eye movements and attention in real-world scenes: the role of global features in object search. *Psychological review*, 113(4):766, 2006.
- [29] J. R. Uijlings, K. E. van de Sande, T. Gevers, and A. W. Smeulders. Selective search for object recognition. *International journal of computer vision*, 104(2):154–171, 2013.
- [30] D. Yoo, S. Park, J.-Y. Lee, A. Paek, and I. S. Kweon. Attentionnet: Aggregating weak directions for accurate object detection. *arXiv preprint arXiv:1506.07704*, 2015.
- [31] C. L. Zitnick and P. Dollár. Edge boxes: Locating object proposals from edges. In *Computer Vision–ECCV 2014*, pages 391–405. Springer, 2014.